Hexagonal boron nitride hollow capsules with collapsed surfaces: Chemical vapor deposition with single-source precursor ammonium fluoroborate*

Xiaopeng Li(李肖鹏)[1], Jun Zhang(张军)[1], Chao Yu(郁超)[1], Xiaoxi Liu(刘晓喜)[1], Saleem Abbas[1], Jie Li(李杰)[1], Yanming Xue(薛彦明)[2,†], and Chengchun Tang(唐成春)[1,‡]

[1] *School of Material Science and Engineering, Hebei University of Technology, Tianjin* 300130, *China*

[2] *World Premier International Center for Materials Nanoarchitectonics (WPI-MANA), National Institute for Materials Science (NIMS), Namiki* 1-1, *Tsukuba, Ibaraki* 305-0044, *Japan*

(Received 10 January 2016; revised manuscript received 25 February 2016; published online 9 June 2016)

SBA-15 (mesoporous SiO_2) is used to stabilize and transfer F^- in the NH_4BF_4 CVD reaction for the first time, and a large-scale crystalline h-BN phase can be prepared. We successfully fabricate hollow h-BN capsules with collapsed surfaces in our designed NH_4BF_4 CVD system. Optimum temperature conditions are obtained, and a detailed formation mechanism is further proposed. The successful SBA-15-assisted NH_4BF_4 CVD route is of importance and enriches the engineering technology in the h-BN single-source CVD reaction.

Keywords: hollow capsule, hexagonal boron nitride, chemical vapor deposition, ammonium fluoroborate

PACS: 81.07.–b, 81.05.Je, 81.15.Gh, 78.30.Hv **DOI:** 10.1088/1674-1056/25/7/078107

1. Introduction

Chemical vapor deposition (CVD) technology is of great importance to fabricate hexagonal boron nitride (h-BN) micro-/nano-materials.[1–5] The traditional plasma-enhanced and thermal CVD technologies are still widely applied to h-BN growth,[6,7] and the most commonly used precursors include multi-source precursors with ammonium (NH_3), such as NH_3–boron halide (BX_3, X = F, Cl, or I), NH_3–boron (B_xH_y), NH_3–organoborane ($R_zB_xH_y$, R = C, F, Cl, or I), NH_3–organoborate [$B(OR)_3$, $R = C_nH_{2n+1}$], etc;[2,8–10] and single-source ones, i.e., some organic or inorganic molecules which contain boron and nitrogen components, for instance, borazine ($B_3N_3H_6$), chloroborazine ($B_3N_3H_{6-x}Cl_x$), ammonia borane (BNH_6), and so on.[5,11–13] Generally speaking, almost all of the multi-source CVD routes possess considerable complexity, and the final h-BN properties depend strongly on the vapor phase composition, the controlled target temperature, and the selective substrate in the reaction system.[5,9–13] In contrast, the single-source precursors can not only make the synthetic route much easier, but also improve the h-BN product.[5,11–13] Actually, both the frequently used single- and multi-source precursor materials are disadvantageous to the controllable CVD routes and the final h-BN micro-/nano-materials because of their deucedly-instable, highly-flammable/explosive, extremely-poisonous, and carbon-contaminated properties.[5,11–13] Furthermore, the above-mentioned single-source materials and their synthetics have been quite costly to date. Therefore, a stable, hazard-free, and carbon-free single-source precursor is highly desirable for the h-BN CVD system, and designing its feasible CVD route is also of great significance for the BN growth technology.

As a commonly-used chemical, ammonium tetrafluoroborate (NH_4BF_4), which is a molecule containing boron and nitrogen, is highly-stable in the ambient atmosphere and very cheap on the market. As reported by Yang *et al.*, a reaction was carried out in an autoclave in the temperature range of 400–600 °C via NH_4BF_4 pyrolysis in metallic Na flux,[14] suggesting that NH_4BF_4 would be able to be used as a single-source precursor in the h-BN CVD system due to its nature of high-temperature sublimation. However, an explosion occurred in the autoclave, easily at such a high temperature in experiments, and it could not be controlled precisely either. $MgCl_2$-assisted NH_4BF_4 CVD was subsequently carried out to successfully obtain a large-scale h-BN phase,[15] indicating the feasibility of using NH_4BF_4 in the single-source CVD reaction. As elaborated in that investigation, the key to h-BN formation in an NH_4BF_4 single-source CVD system is to stabilize the by-product HF generated from the NH_4BF_4 decomposition. Due to the chemical-cycled equilibrium, cycle reaction of NH_4BF_4 occurs in the high-temperature phase ($NH_4BF_4 \rightarrow HF + NH_3BF_3$; $4NH_3BF_3 \rightarrow BN + 3NH_4BF_4$; $4HF + BN \rightarrow NH_4BF_4$), revealing that h-BN formation only happens by effectively depressing the HF content in the reaction zone. The HF can be efficiently limited by forming a stable MgF_2 phase (via

*Project supported by the National Natural Science Foundation of China (Grant Nos. 51332005, 51372066, 51172060, 51202055, and 21103056).

†Corresponding author. E-mail: XUE.Yanming@nims.go.jp

‡Corresponding author. E-mail: tangcc@hebut.edu.cn

© 2016 Chinese Physical Society and IOP Publishing Ltd

a reaction of HF with $MgCl_2$ vapor), resulting in the chemical equilibrium towards h-BN direction and forming h-BN in large-scale. Unfortunately, other chemicals that could play a similar role as $MgCl_2$ have not yet been found or reported for the NH_4BF_4 CVD system.

In this study, mesoporous SiO_2 (SBA-15) is utilized to effectively stabilize and transfer the HF in the single-source NH_4BF_4 CVD reaction system. As a result, a hollow-capsular h-BN structure is successfully obtained. The formation mechanism is proposed for the first time.

2. Experiment

2.1. Material synthesis and characterization

To obtain SBA-15, the mixture of tetraethoxysilane (TEOS) and P123 ($EO_{20}PO_{70}EO_{20}$, Sigma-Aldrich) was stirred at room temperature in a dilute hydrochloric acid solution (pH $<$ 1) for 20 h. The solid product was collected, washed, and air-dried at room temperature. Then the obtained product was calcined at 500 °C for 6 h.[16]

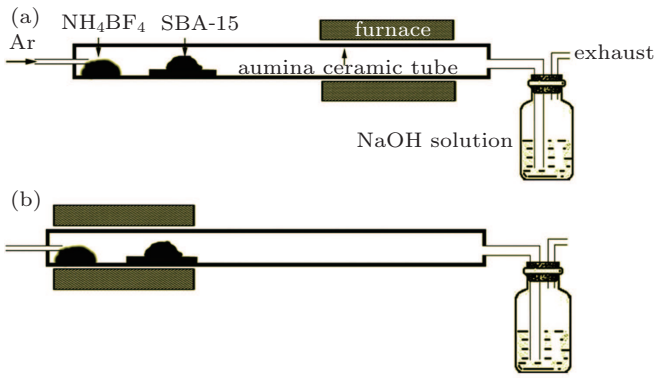


Fig. 1. (color online) Schematic diagram of the CVD system of NH_4BF_4: (a) the system in the heating-up stage; (b) the system in the stable target-temperature stage.

The designed CVD reaction based on NH_4BF_4 in the presence of SBA-15 was carried out in a conventional furnace equipped with a horizontal alumina-ceramic tube (Fig. 1). The ammonium fluoroborate (NH_4BF_4) ($\sim$ 5 g, Tianjin Jiangtian Chemical Technology Co., LTD.) was placed near to the intake of Ar while the SBA-15 ($\sim$ 1 g) was placed next to NH_4BF_4 on an alumina-ceramic plate. The distance between them was about 15 cm. At the beginning, these two materials were far away from the heating area (Fig. 1(a)). The Ar flow was kept constant at 20 ml/min in the whole process. When the system reached to the target temperature, the alumina tube along with the reactants was immediately moved to the heating zone (Fig. 1(b)). It was held at the steady target temperature for 1 h, then cooled to room-temperature naturally. All the toxic exhausts during the reaction were absorbed by a sodium hydroxide solution (NaOH). The final product was collected from the alumina-ceramic plate, and a further removal of SiO_2 was carried out by using a 14 M NaOH solution.

2.2. Characterization

X-ray powder diffraction (XRD) was recorded by a Japan SmartLab Rigaku XRD diffractometer with Cu K radiation (0.154181 nm). The scanning electron microscopy (SEM) and transmission electron microscopy (TEM) images were taken with Japan Hitachi S-4800 field-emission SEM (FE-SEM) (3 kV, resolution $\sim$ 10 nm) and USA TECNAI20 TEM instruments (200 kV, resolution $\sim$ 0.2 nm), respectively. The Fourier transform infrared spectra (FTIR) were measured by using a Germany Bruker OPUS 80V FTIR spectrometer. The Brunauer–Emmett–Teller (BET) parameters and nitrogen–adsorption-desorption isotherms were obtained from a USA Quanta chrome-Instruments 1900 automated-gas-sorption analyzer (77 K).

3. Results and discussion

After the NH_4BF_4 CVD process (at 1050 °C), the as-collected residues exhibit the collapsed surfaces that differed from the smooth ones of raw SBA-15, as shown in Figs. 2(a) and 2(b). The thickness of the obtained hollow-capsular h-BN is about 1 μm, as shown in Fig. 2(b). Actually, the coarse and collapsed surface is composed of numerous disordered ultra-thin sheets (Fig. 2(c)). The clearly visible edges of the super-thin nanosheets are displayed in twists and turns (Fig. 2(d)).

Further TEM measurements indicate that the washed samples completely convert to hollow capsular microstructures from the pristine solid micro-capsules (unwashed) (Figs. 3(a)–3(c)). The detailed HRTEM images reveal the wall of the hollow structure made up of several layers that are $\sim$ 0.34 nm separated from each other (Fig. 3(d) and its inset), and collapsed-morphology nanosheets possessing less than 10 layers (Fig. 3(e), the inset shows a 6-layered nanosheet, single-

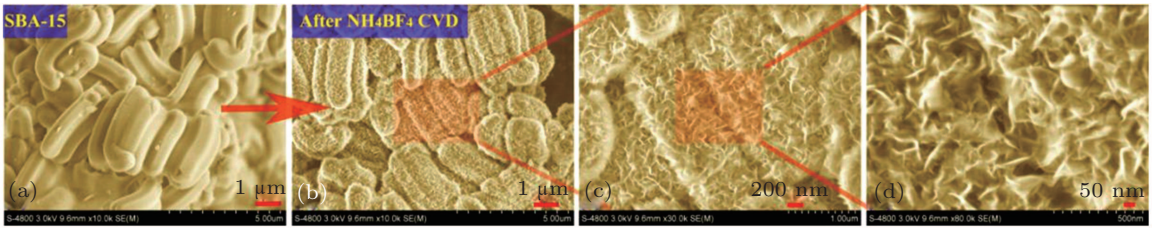


Fig. 2. (color online) SEM images of (a) SBA-15 and (b)–(d) the samples obtained after NH_4BF_4 CVD reaction.

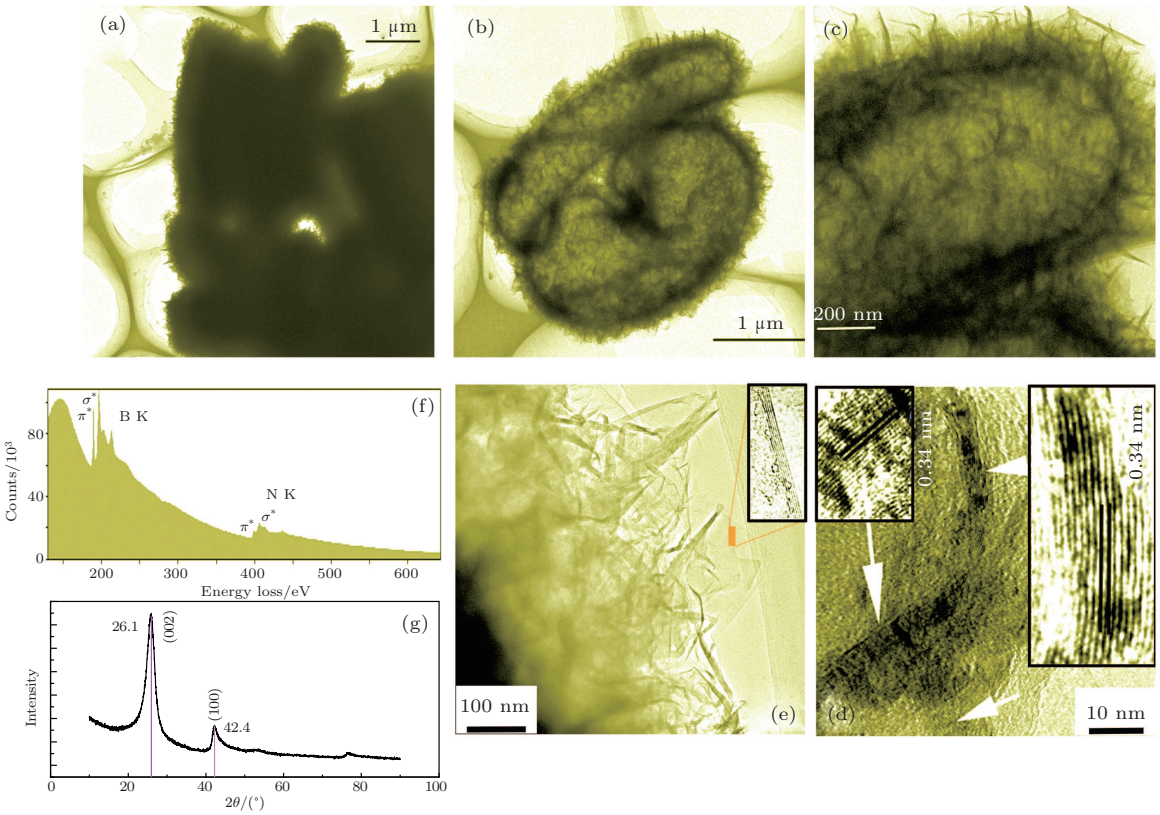


Fig. 3. (color online) Characterization of the samples obtained at 1050 °C: (a) TEM image of the sample without washing by NaOH solution, (b) and (c) TEM images of the sample after washing; (d) and (e) HRTEM images of the sample in (c); (f) EELS spectrum of the washed sample; and (g) XRD pattern of the washed sample.

layered nanosheets can be found frequently). The corresponding EELS analysis demonstrates a nearly 1/1 molar ratio of B/N; no other element was detected (Fig. 3(f)). The XRD pattern can be indexed into the h-BN phase with (002) and (100) planes located at $2\theta = 26.1°$ and 42.4°, respectively. The distance between the (100) and (002) (Fig. 3(g)) planes is calculated to be ~ 0.34 nm by $2d\sin\theta = n\lambda$. Therefore, the as-indexed 0.34 nm distance (inset of Fig. 3(d)) can be assuredly speculated as being the interplanar spacing of the h-BN (002) plane family.[17–22]

In order to obtain the optimum temperature, we did a lot of work. From the XRD patterns of different-temperature samples, we know that the optimum temperature should be fixed at 1050 °C in our experiments, in light of a completely-washed-removal SiO_2 treatment for the relatively pure h-BN (Fig. 4). The XRD patterns illustrate the crystal variations of promoter SBA-15 in the NH_4BF_4 CVD reaction at different temperatures, and reveal the crystal phase of the hollow capsule structure, as shown in Fig. 4. It is clear that two diffraction peaks centered at 25.88° and 42.13° become more and more obvious with increasing temperature. The washed samples have the two peaks at $\sim 26.05°$ and 42.22°, as shown in Fig. 4(b), which are indexed into h-BN lattice planes (002) and (100), respectively (Fig. 4(a)). At 1100 °C, the sharp diffraction peaks that are attributed to SiO_2 crystallization from its amorphous state are observed due to the elevated temperature near the SiO_2 melting point. After an identical washing process by using a concentrated NaOH solution, h-BN crystal phase is determined, especially for the samples fabricated at 1050 °C (without impurity peaks found) (Fig. 4(b)), revealing the obtained samples with a hollow capsule structure corresponding to a pure h-BN phase.

In Fig. 5, we can see that when the set temperature is between 800 °C and 850 °C, the ultrathin h-BN deposits on mesoporous SiO_2 surfaces to form thin nanolayers with smooth surfaces, especially the washed samples have smooth surfaces. Due to HF corroding the as-formed wall layers in the relative high temperature range of 900–950 °C, a handful of nanosheets start to grow along the layered-wall breakages. When the temperature is in the range of 1000–1050 °C, the decomposed HF erodes the formed h-BN surface layers seriously, resulting in more collapsed breakages on the surface. The h-BN growth occurs along the fracture edges by a CVD process of $NH_3{\cdot}BF_3$ [$(4NH_3{\cdot}BF_3(v)+3SiO_2(s)\rightarrow BN(s)+3SiF_4(v)+6H_2O(v)$], leading to a disordered surface with a dense few-layered h-BN structure. When the temperature is higher than 1100 °C, the amorphous SiO_2 is crystallized rapidly before the deposition starts, resulting in numerous broken surfaces.

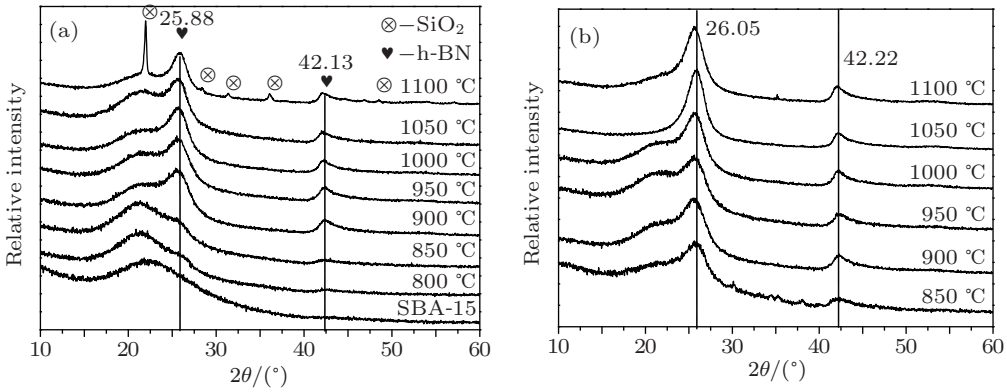


Fig. 4. XRD patterns of the samples: (a) SBA-15 treated with the gaseous ammonium fluoroborate at different temperatures; (b) the corresponding samples with identical washing process by concentrated NaOH solution.

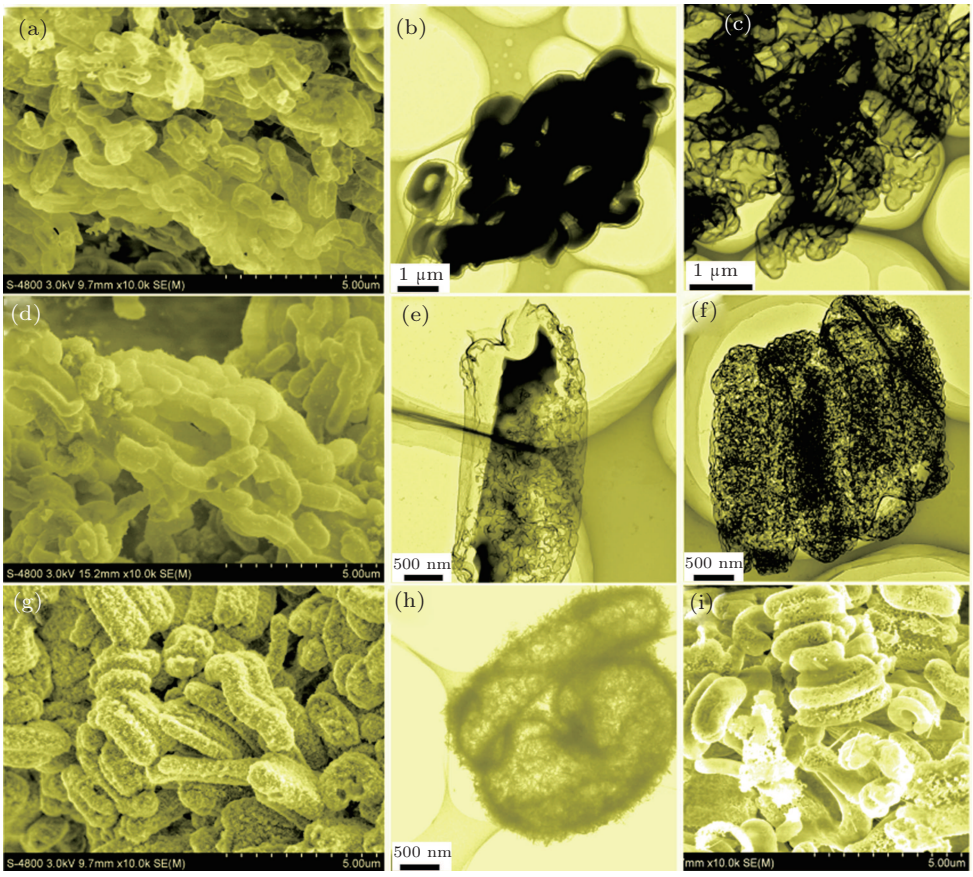


Fig. 5. (color online) SEM and TEM images of the samples obtained at different temperatures: (a), (d), and (g) SEM, temperature in the ranges of 800–850 °C, 900–950 °C, and 1000–1050 °C, the washed samples; (b) and (c) TEM, temperature in the range of 800–850 °C, the unwashed and washed samples; (e) and (f) TEM, temperature in the range of 900–950 °C, the washed samples; (h) TEM, temperature in the range of 1000–1050 °C, the washed samples; (i) SEM, the unwashed samples obtained at 1100 °C.

Figure 6(a) shows the XRD patterns of raw SBA-15, unwashed, and washed samples. The swell-like single peak (centered at $\sim 22.09°$) in the SBA-15 pattern reveals its amorphous property. The washed sample is indexed into h-BN pure phase and the indexed (002) peak is located at $\sim 2\theta = 26.10°$. The unwashed one has mixed phases composed of amorphous SiO_2 (SBA-15) and h-BN (see inset in Fig. 6(a), abbreviated as BN/SiO_2). The FTIR further confirms that the hollow capsules with collapsed surfaces are pure h-BN, as shown in Fig. 6(b). Excluding the two typical h-BN vibration bands (centered at 1387 cm^{-1} and 808 cm^{-1}),[17,23] many additional bands ($\sim$ 3415 cm^{-1}, 2970 cm^{-1}, 2887 cm^{-1}, 1087 cm^{-1}, 1051 cm^{-1}, and 465 cm^{-1}, in the unwashed sample) are attributed to the related SBA-15 (amorphous SiO_2) vibration bands (–OH, $–CH_2$, Si–O–Si, and Si–O–C, corresponding to the C, B, and A frame areas in Fig. 6(b)).[24] These results correspond to the mixed phases (BN/SiO_2) found in the unwashed sample, and the washed one (only two vibration bands located at 1387 cm^{-1} and 808 cm^{-1}) again demonstrates the highly-pure h-BN property. The BET nitrogen adsorption–desorption iso-

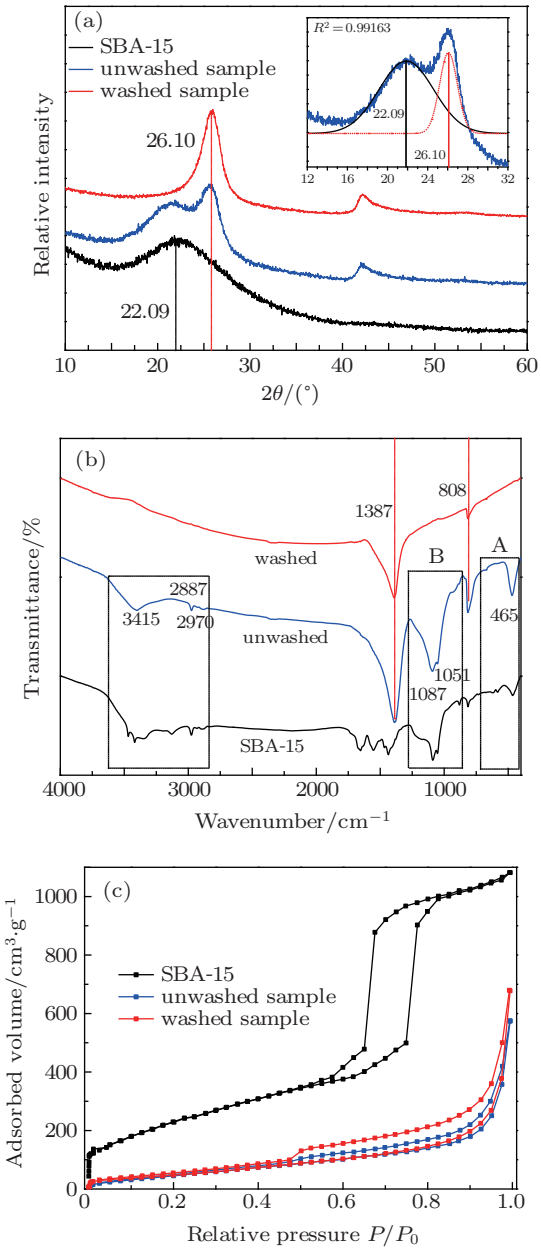


Fig. 6. (color online) (a) XRD patterns, (b) FTIR, and (c) nitrogen adsorption-desorption isothermals of the SBA-15, washed, and unwashed samples obtained at 1050 °C. The inset in panel (a) shows the bimodal fitting.

therm analyses of the samples (obtained at 1050 °C) and raw SBA-15 are also comparatively shown in Fig. 6(c). According to the International Union of Pure and Applied Chemistry (IUPAC) classifications, the isotherm of SBA-15 is attributed to type H1 hysteresis loop, which is associated with porous properties corresponding to well-defined cylindrical-like pore channels. Contrastively, isotherms of the washed and unwashed samples are attributed to the H3 type, indicating a non-rigid aggregation of plate-like particles that can give rise to numerous slit-shaped pores in their aggregation matrix. The BET specific surface area of the hollow capsule is 151 m^2/g, which is far below that of SBA-15 (832 m^2/g), but slightly above that of the unwashed one (134 m^2/g). Thus, the specific surface areas are sharply decreased due to the raw ordered pore channels being seriously destroyed in SBA-15 itself.

The formation mechanism is proposed and demonstrated in Fig. 7. For the NH_4BF_4-cycle reaction, NH_4BF_4 sublimation and decomposition occur simultaneously at high temperature

$$NH_4BF_4(v) \rightarrow NH_3 \cdot BF_3(v) + HF(v). \quad (1)$$

The formed $NH_3{\cdot}BF_3$ vapor not only has a high thermal stability, but also works well as a CVD precursor for h-BN formation[15]

$$4NH_3 \cdot BF_3(v) \rightarrow BN(s) + 3NH_4BF_4(v). \quad (2)$$

However, the decomposed HF by-product can strongly corrode the pre-formed BN, especially at a relatively high temperature (the as-formed BN can be completely consumed by HF), again generating NH_4BF_4

$$BN(s) + 4HF(v) \rightarrow NH_4BF_4(v). \quad (3)$$

Therefore, the chemical vapor balance by the cycle reactions (Eqs. (1)–(3)) leads to a final conclusion that NH_4BF_4 cannot be used as a single-source precursor for the h-BN CVD route. Actually, the formed HF in the reaction balance strongly restricts the BN formation in this CVD reaction. Here, the mesoporous SiO_2 (SBA-15) can effectively stabilize and transfer the HF due to the following related chemical reaction:

$$4HF(v) + SiO_2(s) \rightarrow SiF_4(v) + 2H_2O(v). \quad (4)$$

In order to verify the SiF_4 generation in the SBA-15-assisted NH_4BF_4 CVD reaction system, we added a water-cooling-trap system (with a plastic bottle) in the exhaust gas before the NaOH-solution-cooling-trap system. When the reaction system cooled to room temperature naturally, the water solution of the plastic bottle was dried to obtain a small quantity of white powder. We tested the EDS of this powder, and found that the Si element emerged (Fig. 8). This result can indirectly verify that the chemical reaction $4HF(v)+SiO_2(s)\rightarrow SiF_4(v)+2H_2O(v)$ occurs in the SBA-15-assisted NH_4BF_4 CVD reaction system.

The as-introduced SBA-15 can disequilibrate the NH_4BF_4-cycle reactions by effectively stabilizing and transferring the formed HF in the cycle process. It is predicted that when the temperature is fixed at 1050 °C, the decomposed HF seriously erodes the formed h-BN surface layers, resulting in more collapsed breakages on the surface while h-BN growth occurs along the fracture edges by a CVD process of $NH_3{\cdot}BF_3$ [proposed as $(4NH_3{\cdot}BF_3(v)+3SiO_2(s)\rightarrow BN(s)+3SiF_4(v)+6H_2O(v)]$, leading to a disordered surface with a dense few-layered h-BN structure. Actually, SBA-15 has acted as an *in-situ* template

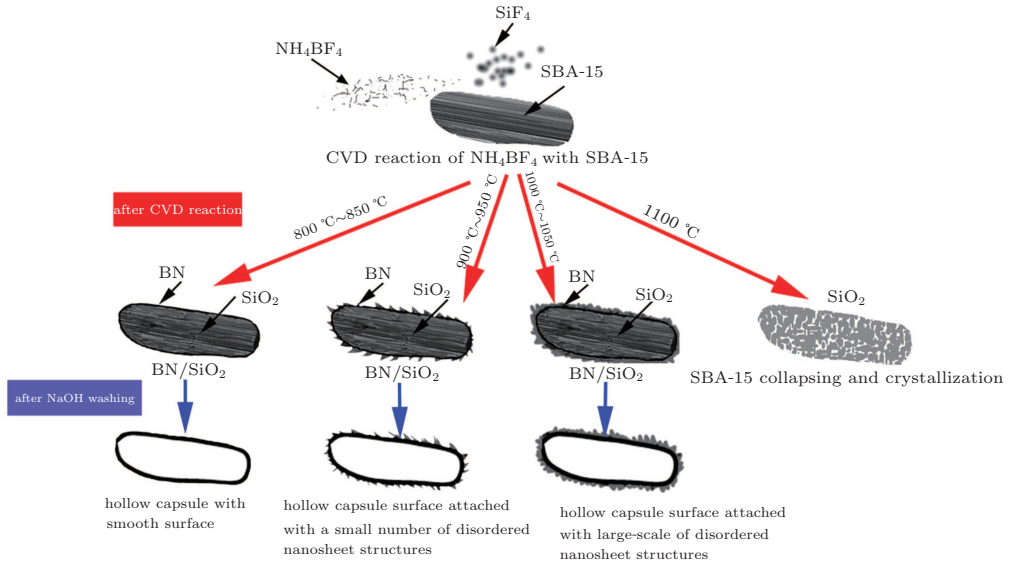


Fig. 7. (color online) Schematic diagram of the formation mechanism.

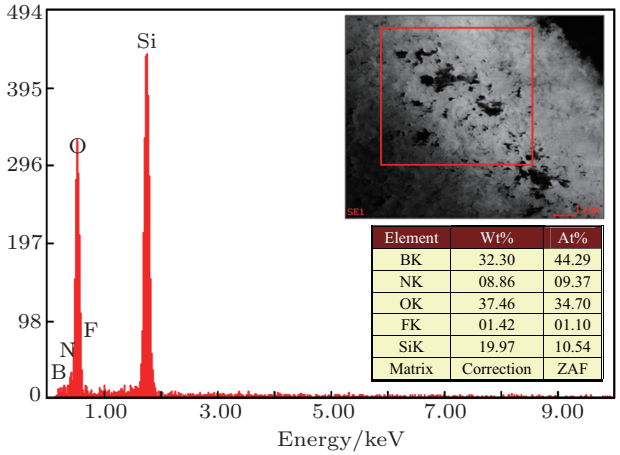


Fig. 8. (color online) EDS of the sample obtained from the water cooling system.

for the h-BN deposition. Although SiF_4 could react with H_2O to generate SiO_2 again [$SiF_4(v)+2H_2O(v)\rightarrow 4HF(v)+SiO_2(s)$], the constant Ar flow could effectively remove SiF_4 and H_2O from the depositing reaction region, which does not influence the h-BN formation on the SBA-15 surfaces. Here, the F^- can be transferred by forming an intermediate SiF_4 in the CVD system, benefiting for the h-BN formation.

4. Conclusion

We successfully synthesized a hollow h-BN capsule structure by using the novel SBA-15-assisted NH_4BF_4 CVD system. The hollow capsule shells were composed of relatively well-aligned h-BN few-layers, and the collapsed surfaces were made up of disordered ultrafine h-BN nanosheets (one-layered and few-layered). The effective F^- stabilization and transference of the HF are vital for h-BN deposition and growth in the NH_4BF_4 CVD reaction.

References

[1] Corso M, Auwärter W, Muntwiler M, Tamai A and Greber T 2004 *Science* **303** 217
[2] Tang C C, Bando Y, Huang Y, Zhi C Y and Golberg D 2008 *Adv. Funct. Mater.* **18** 3653
[3] Liu M X, Zhang Y F and Liu Z F 2015 *Acta Phys. Sin.* **64** 078101 (in Chinese)
[4] Shi Y M, Hamsen C, Jia X T, Kim K K, Reina A, Hofmann M, Hsu A L, Zhang K, Li H N, Juang Z Y, Dresselhaus M S, Li L J and Kong J 2010 *Nano Lett.* **10** 4134
[5] Kim K K, Hsu A, Jia X T, Kim S M, Shi Y M, Hofmann M, Nezich D, Nieva J F R, Dresselhaus M, Palacios T and Kong J 2012 *Nano Lett.* **12** 161
[6] Sugino T and Tai T 2000 *Jpn. J. Appl. Phys.* **39** L1101
[7] Leparoux M and Vandenbulcke L 1999 *J. Am. Ceram. Soc.* **82** 1187
[8] Tsuda O, Watanabe K and Taniguchi T 2010 *Diam. Relat. Mater.* **19** 83
[9] Komatsu S, Kazami D, Tanaka H, Shimizu Y, Moriyoshi Y, Shiratani M and Okada K 2006 *Appl. Phys. Lett.* **88** 151914
[10] Sachdev H, Müller F and Hüfner S 2011 *Angew. Chem. Int. Edit.* **50** 3701
[11] Demin V N, Asanov P and Akkerman Z L 2000 *J. Vac. Sci. Technol. A* **18** 94
[12] Phani A R 1999 *J. Mater. Res.* **14** 829
[13] Gao Y, Ren W C, Ma T, Liu Z B, Zhang Y, Liu W B, Ma L P, Ma X L and Cheng H M 2013 *ACS Nano* **7** 5199
[14] Yang Z H, Shi L, Chen LY, Gu Y L, Cai P J, Zhao A W and Qian Y T 2005 *Chem.Phys. Lett.* **405** 229
[15] Tang C C, Bando Y, Shen G Z, Zhi C Y and Golberg D 2006 *Nanotechnology* **17** 5882
[16] Zhao D, Feng J, Huo Q, Melosh N, Fredrickson G H, Chmelka B F and Stucky G D 1998 *Science* **279** 548
[17] Yuan S, Toury B, Journet C and Brioude A 2014 *Nanoscale* **00** 1
[18] Li J, Xiao X, Xu X W, Lin J, Huang Y, Xue Y M, Jin P, Zou J and Tang C C 2013 *Sci. Rep.* **3** 3208
[19] Nazarov A S, Demin V N, Grayfer E D, Bulavchenko A I, Arymbaeva A T, Shin H J, Choi J Y and Fedorov V E 2012 *Chem. Asian J.* **7** 554
[20] Kubota Y, Watanabe K, Tsuda O and Taniguchi T 2007 *Science* **317** 932
[21] Wang L C, Shen L L, Xu X H, Xu L Q and Qian Y T 2012 *RSC Adv.* **2** 10689
[22] Ma X K, Lee N H, Oh H J, Jung S C, Lee W J and Kim S J 2011 *J. Cryst. Growth* **316** 185
[23] Xue Y M, Elsanousi A, Fan Y, Lin J, Li J, Xu X W, Lu Y, Zhang L, Zhang T T and Tang C C 2013 *Solid State Sci.* **24** 1
[24] Azimov F, Markova I, Stefanova V and Sharipov K 2012 *J. Univ. Chem. Technol. Metallurgy* **47** 333